

Hyaluronic Acid After Subcutaneous Injection—An Objective Assessment

VERENA SANTER, PHARM^{D,*} SAMUEL GAVARD MOLLIARD, MSc,[†] PATRICK MICHEELS, MD,[‡] SERGIO DEL RÍO-SANCHO, PhD,^{*} PIERRE QUINODOZ, MD,[§] YOGESHVAR N. KALIA, PhD,^{*} AND DENIS SALOMON, MD^{||}

BACKGROUND Hyaluronic acid (HA) fillers are the preferred injectable products for aesthetic correction of skin depressions and restoration of facial volume.

OBJECTIVE To investigate the subcutaneous distribution of 3, biophysically distinct, CE-marked and FDA-approved HA fillers.

MATERIALS AND METHODS BEL_B, JUV_V, and RES_L were injected ex vivo in porcine and human skin. Immediately after injection, the skin samples were snap-frozen, cross-sectioned, and visualized using stereomicroscopy and full-field optical coherence tomography. Images were compared with histological sections after hematoxylin and eosin staining.

RESULTS Hyaluronic acid fillers were distributed as homogeneous bolus in the ex vivo skin. The injection bulks were found to preserve the fibrous trabecular network, shift the fat lobules, and displace the adjacent adipocyte layers independently of the formulation injected.

CONCLUSION For the first time, the subcutaneous injection of 3 HA fillers with markedly different biophysical properties was systematically investigated by complementary visualization techniques. Despite their different properties, no difference in distribution was found after subcutaneous injection. The global preservation of the hypodermis structure observed was consistent with the good tolerability seen in clinical practice after implantation of the HA fillers in the subcutaneous skin layer.

The authors have indicated no significant interest with commercial supporters.

The biocompatibility, versatility, and unique biophysical properties of hyaluronic acid (HA) fillers have made them increasingly popular products for soft-tissue correction and volume-restoring procedures.¹ Statistics from the American Society for Aesthetic Plastic Surgery show that injection of HA fillers was the second most practiced nonsurgical procedure in the United States, with more than 2.4 million interventions in 2016.²

Hyaluronic acid fillers are designed by manufacturers for injection either into the dermal layer, in the case of the superficial products, or into the subcutaneous skin layer and the supraperiostic zone for the so-called

“volumizer products.” The behavior of HA gel fillers after intradermal injections has been extensively reported^{3–7} evidencing the high tolerability of the HA fillers with preservation of the dermal cells and the extracellular matrix. The intradermal distribution of the HA fillers was found to depend on their biophysical properties, that is, their viscoelastic properties^{8,9} and their cohesivity levels.¹⁰ Hyaluronic acid fillers with a high cohesivity and low viscoelasticity showed a rather homogeneous integration in the dermis, whereas HA fillers with a poor cohesivity and a high viscoelasticity revealed a more heterogeneous dermal integration.^{3,4} However, although reports have demonstrated the feasibility of intradermal injection of HA

**School of Pharmaceutical Sciences, University of Geneva and University of Lausanne, Geneva, Switzerland; †Kylane Laboratoires SA, Geneva, Switzerland; ‡Private Practice, Geneva, Switzerland; §Hopital de la Tour, Geneva, Switzerland; ||CIDGE International Dermatology Clinic, Geneva, Switzerland*

© 2018 by the American Society for Dermatologic Surgery, Inc. Published by Wolters Kluwer Health, Inc. All rights reserved.
ISSN: 1076-0512 • Dermatol Surg 2019;45:108–116 • DOI: 10.1097/DSS.0000000000001609

fillers by expert injectors (e.g., corroboration through the “blanching” technique developed by Micheels and colleagues by ultrasound imaging),^{5,11} clinical experience, observation of current injection techniques, and physical constraints (e.g., dimensions of a 30G needle) suggest that most injections are directed into the subcutaneous skin layer and not into the dermis—despite the product claims and indications.¹² In this regard, Arlette and Trotter showed that the predominant localization of HA fillers injected for the treatment of nasolabial folds was indeed within the subcutaneous tissue. Given that excellent cosmetic results were nevertheless obtained, it was concluded that the dermal localization of the HA filler products was not a condition sine qua non for the treatment of this common indication.¹³ In contrast to the reports on the distribution of HA fillers in the dermis, little is known about the behavior of HA fillers in subcutaneous fat; this is paradoxical because this is where they are most likely to be found after injection. A recent preliminary investigation described the subcutaneous injection of 2 volumizer HA fillers into a female subject scheduled for abdominoplasty and showed that the product with the highest cohesivity seemed to better maintain gel integrity and homogeneity in the hypodermis, which was consistent with results obtained in the dermis.¹⁴

Given the scarcity of literature on the behavior of HA fillers in the subcutaneous space, the aim of this study was to make a rigorous and systematic assessment of the subcutaneous distribution of 3 CE-marked and FDA-approved HA fillers: Belotero Balance (BEL_B), Juvéderm Voluma with Lidocaine (JUV_V), and Restylane Lidocaine (RES_L). We would emphasize that although not all these products are indicated for subcutaneous implantation, they were chosen to cover a broad spectrum of biophysical characteristics (Table 1).^{8,10,15}

As can be clearly seen in Table 1, BEL_B and RES_L represented the extreme opposites in terms of cohesivity levels, rheological properties (elasticity in shear stress conditions and static compression), and HA gel structures. BEL_B was reported as a highly cohesive and low viscoelastic HA filler, whereas RES_L as a poorly cohesive and highly viscoelastic HA filler; JUV_V was selected as a HA filler with intermediate biophysical properties in comparison with BEL_B and RES_L.

The focus of the study was on the elucidation of the subcutaneous distribution of these commercially available gels at time zero, that is, immediately after subcutaneous implantation in 3 different ex vivo skin

TABLE 1. Summary of the Main Biophysical Properties of the HA Fillers Investigated in This Study

| Properties | BEL _B | JUV _V | RES _L |
|--|--|--------------------------------------|--|
| Cross-linking technology | CMP | Vycross | NASHA |
| Cross-linker | BDDE | BDDE | BDDE |
| HA content (mg/mL) ¹⁵ | 22.5 | 20 | 20 |
| Indication based on CE marking | Indicated to fill moderate facial wrinkles and folds | Indicated to restore facial volume | Indicated for the correction of wrinkles |
| Implantation depth based on CE marking | Dermis | Subcutis and/or suprapariosteal zone | Dermis |
| Cohesivity level according to the Gavard-Sundaram cohesivity scale ¹⁰ | Cohesivity score = 5 (=fully cohesive) | Cohesivity score = 2 (=dispersed) | Cohesivity score = 1 (=fully dispersed) |
| Elasticity G' (Pa) at 0.7 Hz (shear-stress conditions) ⁸ | 63 ± 3 | 314 ± 5 | 677 ± 13 |
| Elasticity E' (Pa) at 0.7 Hz (compression conditions) ⁸ | 31,457 ± 1132 | 41,747 ± 947 | 8456 ± 256 |
| Normal force F _N (N) at 1.5 mm (static compression) ⁸ | 0.51 ± 0.02 | 0.33 ± 0.02 | 0.23 ± 0.01 |
| HA gel macrostructure (optical microscope) ¹⁵⁻¹⁷ | “Spider-web”-like | Particulate | Particulate |
| HA gel microstructure (cryo-SEM) ^{15,18} | Fibrous network | Fibrous network | Fibrous network |

BDDE, butanediol diglycidylether; BEL_B, Belotero Balance; CMP, cohesive polydensified matrix; HA, hyaluronic acid; JUV_V, Juvéderm Voluma with Lidocaine; NASHA, non-animal stabilized hyaluronic acid; RES_L, Restylane Lidocaine.

models: (1) porcine ear skin, (2) human skin samples from abdominoplasty, and (3) human skin samples from facial lifting. Hyaluronic acid distribution in the hypodermis was visualized with the help of 3 complementary imaging techniques: macroscopic observation (using a stereomicroscope), full-field optical coherence tomography, and histological analysis of the injection area to identify eventual characteristic distribution patterns of the HA fillers under investigation.

Materials and Methods

Three CE-marked and FDA-approved HA fillers were purchased from commercial sources: Belotero Balance (BEL_B) manufactured by Merz Pharma (Geneva, Switzerland), Juvéderm Voluma with Lidocaine (JUV_V) manufactured by Allergan (Pringy, France), and Restylane Lidocaine (RES_L) manufactured by Galderma (Uppsala, Sweden). Isopentane and formaldehyde for the snap-freezing and conservation of the skin samples were bought from Sigma-Aldrich (Steinheim, Germany).

The porcine ears from 6-month old pigs (100–120 kg) were obtained from a local slaughterhouse (CARRE, Rolle, Switzerland). Human skin samples from facial liftings (5 subjects) and abdominoplasties (5 subjects) were kindly provided by the private Hôpital de La Tour (Geneva, Switzerland). The use of the human tissues was approved by the ethical committee for clinical and ambulatory research (Association des Médecins du canton de Genève; AMG, protocol 10–25).

Ex Vivo Subcutaneous Injections and Visualization

Porcine Ear Skin Versus Human Skin

Porcine ears were chosen for this study given the anatomical and structural similarity to human skin. A further rationale for choosing this model was the possibility to inject the investigated HA fillers into the hypodermis of the intact porcine ear; this enabled the physiological tension of the tissue to be maintained. This was not possible for the human skin samples, which were harvested after abdominal and

facial interventions and therefore lacked basal and lateral fixation.

Obviously, the facial skin samples were the closest to reality given that, in clinical practice, most HA gel injections are administered to the face. However, the small sizes (i.e., area and volume) of the sample specimens hampered the execution of the subcutaneous injections. Skin samples from the temple area were used because of the presence of significant fat tissue, accepting the presence of thick cranial hair shafts in the images. By contrast, abdominal skin samples did not have these limitations—samples were larger, and subcutaneous fat was abundant, moreover only villous hairs were found.

Subcutaneous Injections and Visualization Techniques

With the aim to use conditions as close as possible to actual treatment, 0.1 mL of each commercial HA filler was injected *ex vivo* through the skin into the subcutaneous fat, by the same expert injector. Needles were used as provided in the commercial product (BEL_B, 30G1/2; JUV_V, 27G1/2; and RES_L, 29G1/2). The injection angle was directed in between 20° and 45° depending on the tissue samples, to ensure that the product was deposited in the hypodermis. For the human abdominal skin, the needle penetration depth was measured to be approx. 6 mm, whereas for porcine skin—as well as the human facial skin samples—more superficial injections with a depth of 2 mm were performed.

After the injection, each sample was isolated and snap-frozen in isopentane chilled with liquid nitrogen (−196°C). In the frozen state, the injection areas were cross-sectioned and immediately observed with a full-field optical coherence tomography (FFOCT) microscope (Light-CT Scanner; LL-Tech, Paris, France) and a stereomicroscope (LEICA S6D, Leica, Heerbrugg, Switzerland).

Full-field optical coherence tomography tissue imaging was of particular interest given the rapidity of sample preparation and the 1-μm resolution of the images.¹⁹ Skin cross-sections were inserted in the FFOCT holder and observed straight away with no

need for complex preparation such as staining that could alter the aspect of the skin. The subcutaneously injected HA gel was not visible directly given its lack of light backscattering properties, whereas the surrounding fat tissue and the upper dermis were clearly defined. Observation of the injection site under the stereomicroscope was used to confirm the presence of the gel in the injection cavity. All samples were then fixed in formaldehyde and submitted for histological slicing in paraffin and staining with hematoxylin and eosin.

Results

Porcine Ear Skin

The injections of the 3 HA fillers were performed in porcine ear skin to visualize the effect of the injection bulk on the surrounding subcutaneous structures and vice versa. Given the tissue attachment present in this

skin model, for example, on the cartilage and/or the muscle, one interesting question was whether this tension would influence the diffusion properties of the HA gels. Injection area cross-sections were immediately observed by FFOCT; the minimal sample preparation enabled the imaging of the skin in an almost native state. As shown in Figure 1, minimal deformation of the hypodermis was observed after the HA gel injections. In FFOCT, the direct visualization of HA fillers was not possible given the absence of contrast of the HA gel; however, complementary observation of the injection area with the stereomicroscope revealed its presence.

From the FFOCT images, it was clear that the fat lobules were displaced, and thus, the adipocytes in the first layers of cells adjacent to the HA gel were shifted but not structurally altered, and this was systematically observed in all of the samples (Figure 2).

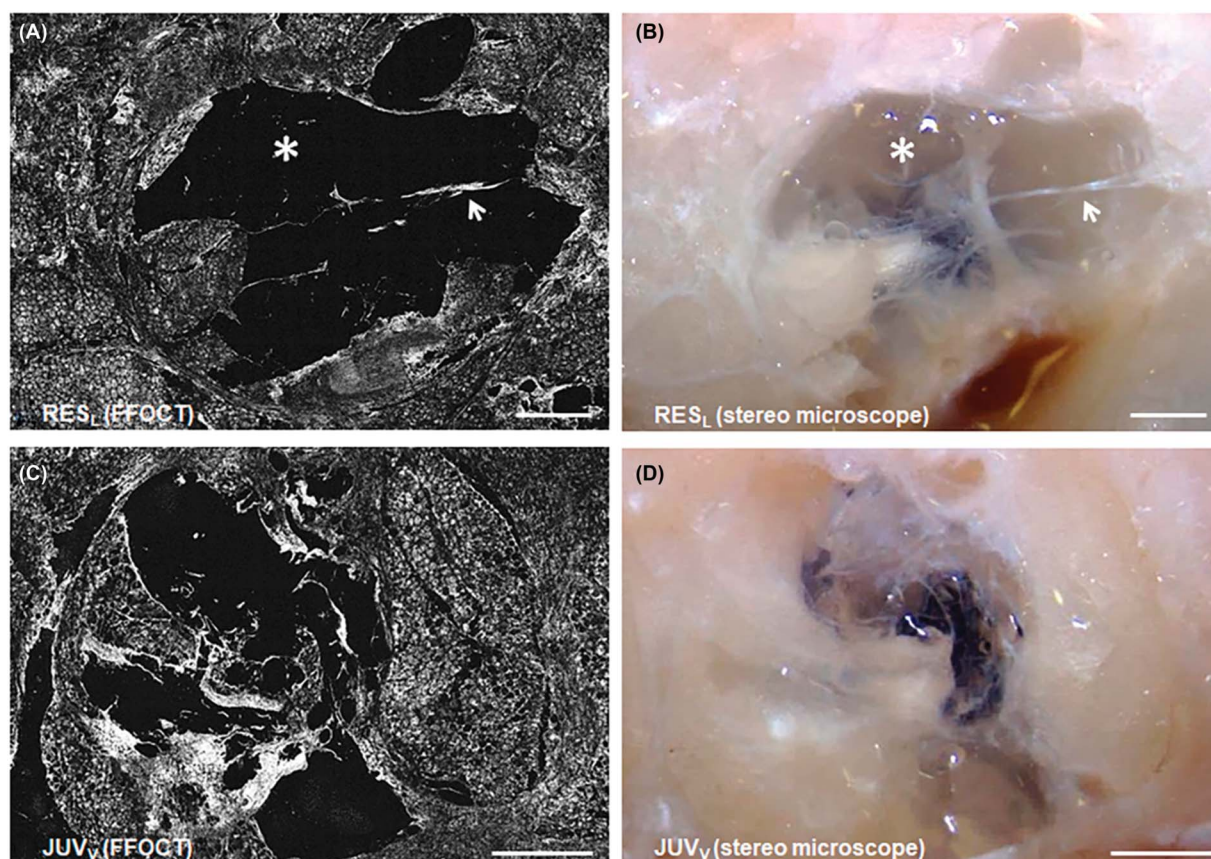


Figure 1. Subcutaneous injection sites of HA fillers (RES_L and JUV_V) in porcine ear skin: (A and C) FFOCT images and (B and D) corresponding stereomicroscope images. For purpose of clarity, HA filler (*) and subcutaneous trabeculae (≧) are indicated. Scale bar = 500 μm. FFOCT, full-field optical coherence tomography; HA, hyaluronic acid; JUV_V, Juvéderm Voluma with Lidocaine.

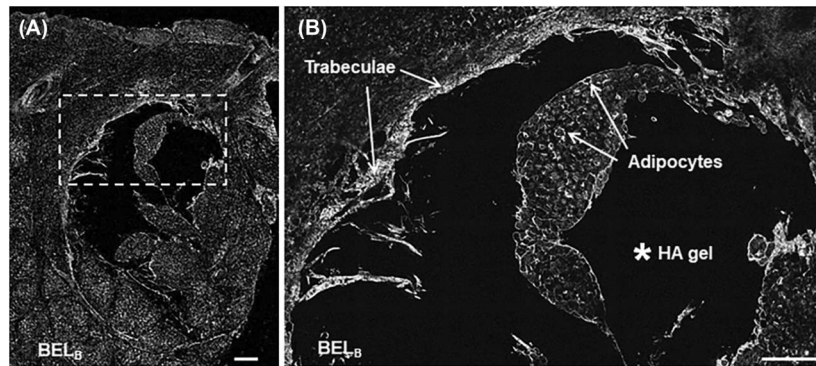


Figure 2. FFOCT images of BEL_B injections into porcine ear hypodermis: (A) cross-section, (B) zoom on upper injection site with focus on the trabeculae fibers and adipocytes. Scale bar = 500 μ m. BEL_B, Belotero Balance; FFOCT, full-field optical coherence tomography; RES_L, Restylane Lidocaine.

Moreover, the interlobular network of trabeculae seemed to surround recurrently the injection site and partially divide the HA gel bolus. As images of the 3 biophysically distinct HA fillers highlighted (Figures 1 and 2), no distinguishable difference between the effects of the gels could be observed. Furthermore, when the injection site was compared with human skin *ex vivo* (Figure 3), no influence of the tissue tension present could be identified, that is, no distinct HA gel distribution was observed.

Human Abdominal Skin

The subcutaneous injection of the HA fillers in human abdominal skin showed similar behavior to the results in porcine ear skin. All 3 HA fillers, injected into the

abdominal subcutaneous fat formed a mainly homogeneous bolus. Figure 3 shows representative images taken with the stereomicroscope of the cross-sections of BEL_B, JUV_V, and RES_L in the abdominal skin fat tissue (n = 5 replicates for each product). Interestingly, comparison of the images shows that the horizontal distribution of the HA gels seemed to be delimited by the interlobular trabeculae (fibrous septa) that cross the fat tissue and link the dermis to the underlying fascia.^{20,21}

The subcutaneous trabecular structure was very clearly delineated after hematoxylin and eosin staining of the samples; macro images and histology slices of the corresponding skin samples are shown in Figure 4.

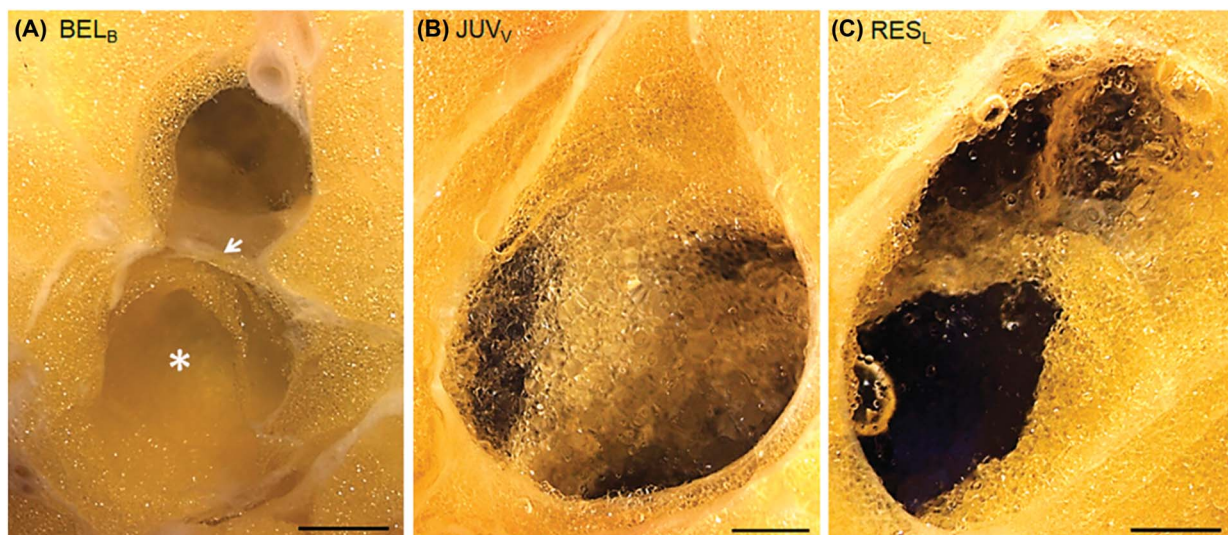


Figure 3. Cross-section macro images after subcutaneous injection into human abdominal hypodermis of (A) BEL_B, (B) JUV_V, and (C) RES_L. For purpose of clarity, HA filler (*) and subcutaneous trabeculae (\geq) are indicated. Scale bar = 1000 μ m. BEL_B, Belotero Balance; HA, hyaluronic acid; JUV_V, Juvéderm Voluma with Lidocaine; RES_L, Restylane Lidocaine.

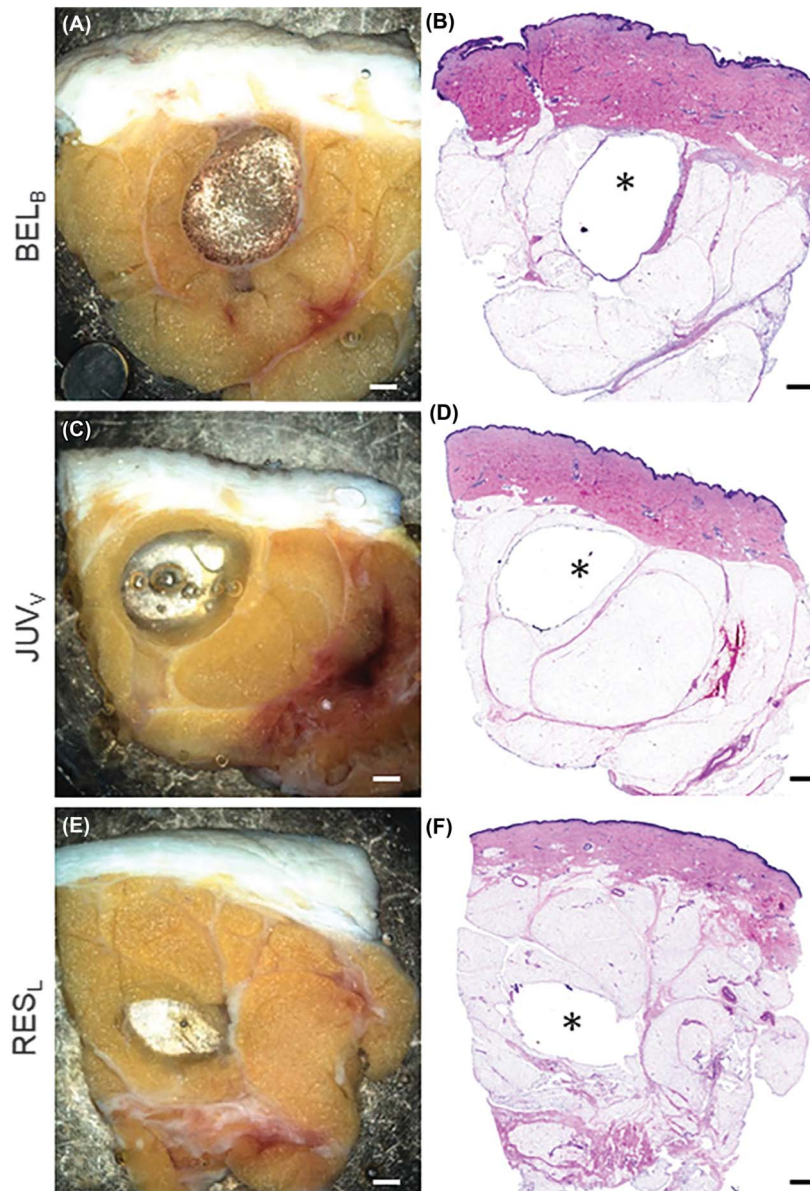


Figure 4. Human abdominal skin subcutaneous injection. Side by side panels show the macro and the corresponding histological images of (A and B) BEL_B, (C and D) JUV_V, and (E and F) RES_L. *The areas corresponding to the HA gel injection sites—during slicing and hematoxylin and eosin staining, most of the gels were eliminated from the samples. Scale bar = 1000 μ m. BEL_B, Belotero Balance; HA, hyaluronic acid; JUV_V, Juvéderm Voluma with Lidocaine; RES_L, Restylane Lidocaine.

It is important to mention that in the histological cross-sections, only very few traces of the HA gels were visible. It was noticed that during the slicing procedure in paraffin—required for preparation of the histological samples—HA gels were eliminated from the lamellae; it seemed that the soft fat tissue was unable to retain the HA gels during processing. This is why it was essential to observe the samples immediately after injection and cross-sectioning with the stereomicroscope, which confirmed the presence of the gels with their “jelly-like” aspect. Comparison of the images of

the same area using the different visualization techniques confirmed that the void spaces seen in the histological slices corresponded to the imprint of the HA gel distribution in the subcutaneous skin layer.

Human Facial Skin

Comparable to the results with human abdominal skin and porcine ear skin, the HA fillers were again distributed in the facial subcutaneous skin mostly as homogeneous boluses that were occasionally confined by the interlobular fibrous septa (trabeculae).

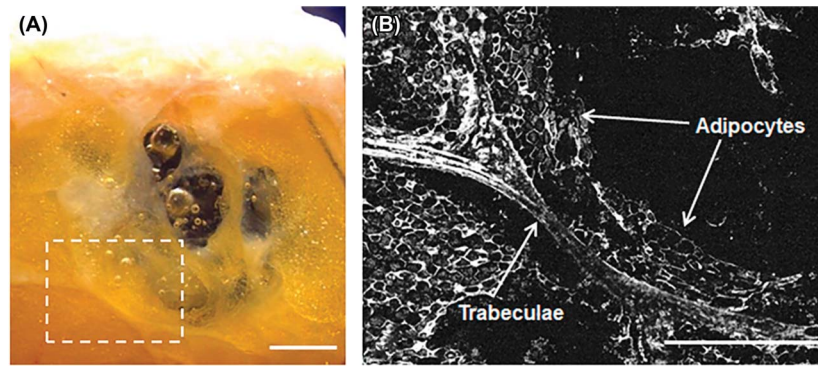


Figure 5. Facial skin subcutaneous injection area of BEL_B: (A) stereo image, (B) FFOCT image with focus on displaced adipocyte layers surrounding the HA filler and the trabecular filament. Air bubbles can clearly be seen in the HA gel in the stereo image. Scale bar = 1000 μm. BEL_B, Belotero Balance; FFOCT, full-field optical coherence tomography; HA, hyaluronic acid.

It was important to note that the fibrous structures of the hypodermis seemed unaltered by the injected HA fillers; only the fat lobules were displaced by the HA

gels, and the first layers of adipocytes adjacent to the gel were shifted. This is evidenced in Figure 5, which shows the macro image of BEL_B injection in the

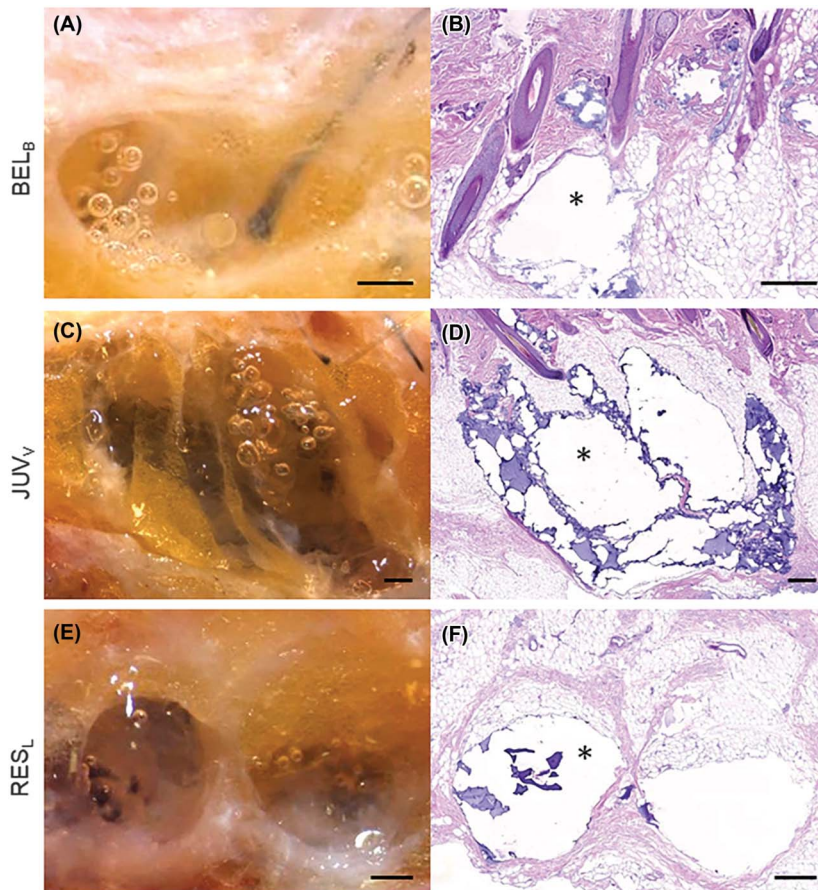


Figure 6. Facial skin images after subcutaneous injections of BEL_B, JUV_V, and RES_L. Images (A, C, and E) show injection site cross-sections under the stereomicroscope, whereas images (B, D, and F) present the corresponding histological slices with hematoxylin and eosin staining. *The empty areas in the histological images of the HA injection bulk, parts of the HA gels were still visible as purple scale-like structures. Scale bar = 500 μm. BEL_B, Belotero Balance; HA, hyaluronic acid; JUV_V, Juvéderm Voluma with Lidocaine; RES_L, Restylane Lidocaine.

temporal subcutaneous fat layer. The detailed image with the FFOCT microscope evidences once more the adipocytes and the proximate trabeculae surrounding the HA gel.

In comparison with abdominal skin, subcutaneous fat was less present, and the connective tissue network was more abundant in facial skin samples. Comparative macro images of injection areas with the corresponding histology images are shown in Figure 6.

Discussion

In this article, for the first time 3 complementary visualization techniques, stereomicroscopy, FFOCT, and histology were used to investigate the subcutaneous distribution of 3 commercially available HA filler formulations. The lower elasticity of the subcutaneous skin as compared to the dermis meant that it did not significantly influence the HA gel distribution. Therefore, the distinct biophysical characteristics of the HA fillers chosen for this study (BEL_B, JUV_V, and RES_L) did not lead to characteristic “product-specific” distribution patterns.

All HA gels seemed to distribute as homogeneous boluses in between the fibrillary network displacing the fat lobules. The subcutaneous trabeculae network was seen to form a resistant envelope, which contains and constrains the HA filler, limiting its movement. On the other hand, HA gel contoured by the quite rigid and undamaged collagenous structures was found to shift and displace the adjacent adipocyte layers.

It is also important to note that no alteration of the trabecular network and/or compression of the fat lobules were evidenced in any of the ex vivo models used. Histological images obtained by hematoxylin–eosin staining revealed the morphological preservation of the cutaneous structure. Although experiments were not designed to detect inflammatory responses (due to the ex vivo nature of the study), the structural integrity of the subcutaneous tissue, that was observed, was consistent with the excellent tolerability of HA fillers in clinical practice.

Acknowledging these findings, it is, however, important to consider the limitations of the present ex vivo

study. First, it was of course not in vivo; the experiments were performed on small excised human skin samples without lateral anchorage. Second, the injected volume of HA filler was 0.1 mL, which is much lower than the total volume that is used in clinical practice. Moreover, due to the immediate processing of the skin samples after injection, HA filler distribution was only observed at time zero; there is no insight into time-dependent effects, in particular, the impact of tissue dynamics and movement that might modify HA filler behavior over time in vivo. Further investigations, with an increased patient and injector number, are obviously required for a better understanding of the behavior of HA filler in vivo over time and when exposed to dynamic conditions and degradation in the skin. Nonetheless, the results presented here constitute a valuable and important first step. Translating these ex vivo data to the “bedside” and what they mean for the clinician, (1) the biomechanical properties of the HA fillers did not seem to affect their distribution in the subcutaneous tissue, which is, more often than not, where they arrive after injection (with the caveat of the lack of time-dependent and/or dynamic effects); (2) this systematic imaging study provides an additional “biophysical” validation of the excellent safety profile of clinical procedures involving injection of HA filler into the subcutaneous skin layer.

Conclusion

Images from this preliminary ex vivo study showed no difference in the subcutaneous integration of BEL_B, JUV_V, and RES_L in porcine ear and human skin samples after injection. This was in contrast to their previously reported behavior in the dermis and the very distinct biophysical properties of the investigated HA fillers. The difference in the resistance of skin layers was believed to be a key given the high elasticity of the dermis in comparison with the “relative inelasticity” of the subcutaneous fat.

For all the investigated HA fillers, the visualization of the injection areas showed the preservation of the hypodermal structure. The fibrous trabecular network was unaltered, and the intercommunicating collagenous trabecular structures seemed to contain and constrain HA filler distribution and limit the

movement of the product. The displacement and compression of the soft fat lobules provided space for HA filler integration into the subcutaneous fat— independent of the formulation injected. The results provide further corroboration of clinical observations concerning the high tolerability of HA filler injections into the hypodermis.

Nevertheless, these findings correspond to static *ex vivo* conditions, which neglect the dynamic mechanical constraints that are constantly applied to an implanted HA filler (e.g., changing facial expression). Further studies to observe the dynamic behavior of HA filler products as a function of time in the subcutaneous skin layer under physiological conditions would be useful to complete the understanding of HA distribution in the hypodermis from injection to product degradation.

Acknowledgments The authors thank the University of Geneva for a teaching assistantship for Verena Santer. The authors acknowledge Dr. Didier Sarazin at the Laboratoire Viollier SA for the preparation of hematoxylin–eosin staining of the skin samples. The authors also thank the CMU bioimaging platform and, in particular, Olivier Brun for help with the wide-field slide scanner microscope for the histological slides. Yogeshvar N. Kalia is extremely grateful to CARIGEST SA for its counsel to an anonymous benefactor for the generous award of a grant to acquire the Light-CT Scanner.

References

1. Fallacara A, Manfredini S, Durini E, Vertuani S. Hyaluronic acid fillers in soft tissue regeneration. *Facial Plast Surg* 2017;33:87–96.
2. The American Society for Aesthetic Plastic Surgery. Procedural statistics. Available from: <https://www.surgery.org/media/statistics>. Accessed July 13, 2017.
3. Flynn TC, Sarazin D, Bezzola A, Terrani C, et al. Comparative histology of intradermal implantation of mono and biphasic hyaluronic acid fillers. *Dermatol Surg* 2011;37:637–43.
4. Tran C, Carraux P, Micheels P, Kaya G, et al. In vivo bio-integration of three hyaluronic acid fillers in human skin: a histological study. *Dermatology* 2014;228:47–54.
5. Micheels P, Sarazin D, Besse S, Sundaram H, et al. A blanching technique for intradermal injection of the hyaluronic acid Belotero. *Plast Reconstr Surg* 2013;132:59s–68s.
6. Micheels P, Besse S, Flynn TC, Sarazin D, et al. Superficial dermal injection of hyaluronic acid soft tissue fillers: comparative ultrasound study. *Dermatol Surg* 2012;38:1162–9.
7. Kohn JC, Goh AS, Lin JL, Goldberg RA. Dynamic high-resolution ultrasound in vivo imaging of hyaluronic acid filler injection. *Dermatol Surg* 2013;39:1630–6.
8. Gavard Molliard S, Albert S, Mondon K. Key importance of compression properties in the biophysical characteristics of hyaluronic acid soft-tissue fillers. *J Mech Behav Biomed Mater* 2016;61:290–8.
9. Sundaram H, Cassuto D. Biophysical characteristics of hyaluronic acid soft-tissue fillers and their relevance to aesthetic applications. *Plast Reconstr Surg* 2013;132:5s–21s.
10. Sundaram H, Rohrich RJ, Liew S, Sattler G, et al. Cohesivity of hyaluronic acid fillers: development and clinical implications of a novel assay, pilot validation with a five-point grading scale, and evaluation of six U.S. food and drug administration-approved fillers. *Plast Reconstr Surg* 2015;136:678–86.
11. Micheels P, Besse S, Sarazin D, Vincent AG, et al. Quantifying depth of injection of hyaluronic acid in the dermis: data from clinical, laboratory, and ultrasound settings. *J Drugs Dermatol* 2016;15:483–90.
12. Arlette JP, Trotter MJ. Anatomic location of hyaluronic acid filler material injected into nasolabial fold: a histologic study. *Dermatol Surg* 2008;34:S56–62.
13. Micheels P, Goodman L. Injection depth in intradermal therapy: update and correction of published data. *J Drugs Dermatol* 2018;17:89–96.
14. Micheels P, Besse S, Sarazin D, Quinodoz P, et al. Ultrasound and histologic examination after subcutaneous injection of two volumizing hyaluronic acid fillers: a preliminary study. *Plast Reconstr Surg Glob Open* 2017;5:e1222.
15. Karine M, Massoud D, Jeremy T, Samuel Gavard M. Influence of the macro- and/or microstructure of cross-linked hyaluronic acid hydrogels on the release of two model drugs. *J Glycobiol* 2016;5:119.
16. Ohrlund JA, Edsman KL. The myth of the “biphasic” hyaluronic acid filler. *Dermatol Surg* 2015;41:S358–64.
17. Micheels P, Sarazin D, Tran C, Salomon D. Effect of different crosslinking technologies on hyaluronic acid behavior: a visual and microscopic study of seven hyaluronic acid gels. *J Drugs Dermatol* 2016;15:600–6.
18. Flynn TC, Thompson DH, Hyun SH, Howell DJ. Ultrastructural analysis of 3 hyaluronic acid soft-tissue fillers using scanning electron microscopy. *Dermatol Surg* 2015;41:S143–S52.
19. Dubois A, Moreau J, Boccara C. Spectroscopic ultrahigh-resolution full-field optical coherence microscopy. *Opt Express* 2008;16:17082–91.
20. Guimberteau JC. Le système multifibrillaire est-il l'architecture structurante de la matrice extracellulaire? *Ann Chir Plast Esthet* 2012; 57:502–6.
21. Wong R, Geyer S, Weninger W, Guimberteau JC, et al. The dynamic anatomy and patterning of skin. *Exp Dermatol* 2016;25:92–8.

Address correspondence and reprint requests to: Denis Salomon, MD, CIDGE International Dermatology Clinic, 14 Quai du Seujet, 1201 Geneva, Switzerland, or e-mail: denis.salomon@cidge.ch